Video Article

Measurement of Aggregate Cohesion by Tissue Surface Tensiometry

Christine M. Butler, Ramsey A. Foty
Department of Surgery, UMDNJ-Robert Wood Johnson Medical School

Correspondence to: Ramsey A. Foty at fotyra@umdnj.edu

URL: http://www.jove.com/details.php?id=2739
DOI: 10.3791/2739
Citation: Butler C.M., Foty R.A. (2011). Measurement of Aggregate Cohesion by Tissue Surface Tensiometry. JoVE. 50. http://www.jove.com/details.php?id=2739, doi: 10.3791/2739

Abstract

Rigorous measurement of intercellular binding energy can only be made using methods grounded in thermodynamic principles in systems at equilibrium. We have developed tissue surface tensiometry (TST) specifically to measure the surface free energy of interaction between cells. The biophysical concepts underlying TST have been previously described in detail[1,2]. The method is based on the observation that mutually cohesive cells, if maintained in shaking culture, will spontaneously assemble into clusters. Over time, these clusters will round up to form spheres. This rounding-up behavior mimics the behavior characteristic of liquid systems. Intercellular binding energy is measured by compressing spherical aggregates between parallel plates in a custom-designed tissue surface tensiometer. The same mathematical equation used to measure the surface tension of a liquid droplet is used to measure surface tension of 3D tissue-like spherical aggregates. The cellular equivalent of liquid surface tension is intercellular binding energy, or more generally, tissue cohesivity. Previous studies from our laboratory have shown that tissue surface tension (1) predicts how two groups of embryonic cells will interact with one another[1-5], (2) can strongly influence the ability of tissues to interact with biomaterials[6], (3) can be altered not only through direct manipulation of cadherin-based intercellular cohesion[7], but also by manipulation of key ECM molecules such as FN[8-11] and 4) correlates with invasive potential of lung cancer[12], fibrosarcoma[13], brain tumor[14] and prostate tumor cell lines[15]. In this article we will describe the apparatus, detail the steps required to generate spheroids, to load the spheroids into the tensiometer chamber, to initiate aggregate compression, and to analyze and validate the tissue surface tension measurements generated.

Protocol

1. Aggregate preparation for measurement of tissue surface tension.

For adherent cells, spheroids can be formed by using either the hanging drop method or by generating a coherent sheet of cells that can then be cut into 1 mm fragments.

Aggregate formation by the hanging drop method:

1. Near-confluent adherent cell cultures should be grown to 90% confluence, whereupon monolayers should be rinsed twice with PBS. After draining well, add 2 mls (for 100 mm plates) of 0.05% trypsin-1 mM EDTA, and incubate at 37°C until cells detach. Stop trypsinization by adding 2 mls of complete medium and gently use a 5 ml pipette to triturate the mixture until cells are in suspension. Transfer cells to a 15 ml conical tube.
2. Add 40 µl of a 10 mg/ml DNAse stock solution and incubate for 5 minutes at RT. Vortex briefly and centrifuge at 200 x g for 5 minutes.
3. Discard supernatant and wash pellet with 1 ml complete tissue culture medium. Repeat, then resuspend cells in 2 mls of complete tissue culture medium.
4. Count the cells using a hemacytometer, or automated cell counter and adjust concentration to 2.5 x 10^6 cells/ml.
5. Remove the lid from a 60 mm tissue culture dish and place 5 mls of PBS in the bottom of the dish. This will act as a hydration chamber.
6. Invert the lid and use a 20 µl pipette to deposit 10 µl drops onto the bottom of the lid. Make sure that drops are placed sufficiently apart so as to not touch. It is possible to place at least 20 drops per dish.
7. Invert the lid onto the PBS-filled bottom chamber and incubate at 37°C/5% CO_2/95% humidity, monitor the drops daily and incubate until either cell sheets or aggregates have formed.
8. Once sheets form, they can be transferred to round-bottom glass shaker flasks containing 3 mls of complete medium and incubated in a shaking water bath at 37°C and 5% CO_2 until spheroids form.

Aggregate formation by the cell sheet method:

9. Single cell suspensions are prepared as described above but concentration is adjusted to 1x10^6 cells/ml.
10. Transfer 3 ml of the cell suspension to 10 ml round-bottom flasks (Belco, Vineland, NJ).
11. Incubate flasks in a gyratory water bath/shaker (New Brunswick Scientific, Edison, NJ) at 37°C, 5% CO_2 for 4h at 120 rpm until cells recover from trypsinization.
12. Transfer cells to a glass round-bottom centrifuge tube and centrifuge at 200 X g into a thin pellet. Incubate for another 24 h until a coherent sheet forms.
13. Gently swirl the culture tube to dislodge the sheet and pour the contents of the culture tube into a small, sterile glass tissue culture dish.
14. Use micro scalpels to cut the sheets into fragments of various sizes.
15. Incubate fragments at 37°C on the gyratory waterbath shaker at 120 rpm under 5% CO_2 for 2 to 3 days or until they become spherical.

2. Measurement of aggregate surface tension

1. **The tissue surface tensiometer**. The apparatus is shown in Figs. 1 and 2. The compression cell (Fig. 3) is composed of two chambers. The outer chamber (OC) is connected to a 37°C circulating water pump, and serves to regulate the temperature of the inner chamber (IC). The chambers are constructed of milled Delrin and contain quartz windows for visualization of the aggregate. The lower assembly (LA) screws

into the base of the inner chamber and is used to 1) position the aggregate in the inner chamber; 2) seal the bottom of the inner chamber; 3) elevate the aggregate to initiate compression; and (4) control the distance between the parallel plates and hence the compression of the aggregate. The central core (CC) of the assembly is adjustable. The tip of the central core (the pedestal) is composed of smooth Teflon and acts as the lower compression plate (LCP). The upper compression plate (UCP) is a Teflon cylinder 15mm long that hangs from the balance arm (B) by a flame-straightened nickel-chromium wire (NCW)*. During the course of an experiment, the cell aggregate (A) is positioned on the lower plate and raised until it contacts the upper plate. The upper plate is connected to the balance arm (B). Compression of the aggregate causes displacement of the balance arm. The balance is a Cahn/Ventron model 2000 recording electrobalance, which operates on the null balance principle. The fulcrum of the balance arm has an armature within a permanent magnetic field. When the balance is operating, it continuously modulates the current passing through the electromagnetic assembly, which in turn maintains the balance arm in the horizontal position. When an object is suspended from the balance arm, the voltage, which the balance applies to keep the arm in the horizontal position, is proportional to the object's weigh. This voltage measures the external compressive force applied to the aggregate. The aggregate's shape is monitored by visual observation through a 25 x Nikon SMZ10A stereoscope coupled to a computer equipped with a frame grabber. In order to minimize adhesion of cell aggregates to the compression plates, both the lower and upper compression plates were coated with poly (2-hydroxyethylmethacrylate) {poly(HEMA)}, a polymeric material to which cells do not adhere [16].
* The wire is flame-straightened by hanging a 15-inch length of wire from a retort stand and clamping a small binder clip to the end. A Bunsen burner is then run up and down the length of the wire until the wire glows red. The straightened wire can then be cut into the appropriate lengths. A small hook is formed by bending the wire approximately ¼ of an inch from the end using two razor blades. The other end is then inserted into the barrel of the lower compression plate.

2. **Aggregate compression.**
    1. The inner chamber is filled with pre-warmed CO_2-independent tissue culture medium (Gibco/BRL, NY).
    2. Aggregates ranging in size from about 200-300 μ are positioned on the lower compression plate (Fig. 4A). Aggregates are loaded by aspirating an aggregate in tissue culture medium half-way up the tip of a Pasteur pipette fitted with a silicone bulb, transferring the pipette to the inner chamber, and positioning the tip of the pipette above the LCP. The aggregate is then gently expelled onto the LCP by gently squeezing the bulb. Alternatively, the aggregate is allowed to fall by gravity onto the LCP.
    3. The upper compression plate (UCP) is positioned above the aggregate and allowed to settle, establishing a pre-compression apparent UCP weight baseline.
    4. The LCP is then raised until the aggregate is compressed against the UCP (Fig. 4B). Adjusting the height of the inner core of the lower apparatus will control different degrees of compression. Compression is monitored by observation through a dissecting microscope equipped with a CCD video camera.
    5. Aggregate images are captured, digitized, and analyzed using ImageJ. Apparent UCP weight change is continuously recorded on a strip chart recorder, achievement of shape equilibrium being denoted by the leveling-off of the Cahn balance's voltage output. Each aggregate is subjected to 2 different degrees of compression.

3. **Calculation of aggregate surface tension.**
    At shape equilibrium, the cohesivity of an aggregate of cells compressed between parallel plates to which it does not adhere can be obtained from the Young-Laplace equation (Fig. 5), where σ is cohesivity, F is the force acting to compress the aggregate, πr_3^2 is the area of the surface of the aggregate upon which force F is exerted, and R_2 and R_3 are, respectively, the radius of the equator of the compressed aggregate and the radius of an arc defining its surface profile normal to the compressing plates and extending between them (Fig. 6). Measuring the compressive force and geometry at force and shape equilibrium and applying these measurements to the Young-Laplace equation generates numerical values of apparent tissue surface tension. Upon reaching equilibrium and calculation of σ_1, aggregates are decompressed and allowed to approach a second equilibrium and σ_2 is calculated as described above.
4. **Confirmation of aggregate liquidity.**
    The calculated surface tension of a liquid aggregate, when subjected to two different compressions will remain constant. In such aggregates the ratio of σ_2/σ_1 will be equal to 1 and will be less than the ratio of the force applied at each successive compression (F_2/F_1). In contrast, the calculated surface tension of an elastic aggregate will obey Hooke's law and increase proportionately to the applied force. For elastic aggregates the ratio of σ_2/σ_1 will not be equal to 1 but will instead approach the ratio of F_2/F_1. The surface tension of liquid aggregates will also be independent of aggregate size [2,17]. Only measurements in which surface tension is independent of the applied force and size are used to calculate average σ for each cell line.

3. Representative results:

Below is a table of typical TST results for aggregates of rat prostate fibroblasts (RPF) and rat prostate smooth muscle cells (RPSMC). As can be seen in Fig. 7 aggregates of RPF cells have a surface tension of 22.8 ± 1.1 dynes/cm. Moreover, the mean surface tension values measured after compression 1 and after compression 2 were statistically identical when compared by a paired t-test. We also compared the ratios of σ_2/σ_1 and F_2/F_1 to ensure that these aggregates did not obey Hooke's law, as they would if they behaved as elastic solids. As demonstrated in Table 1, the ratio of σ_2/σ_1 does indeed approach 1.0. Moreover, the ratio of F_2/F_1 was significantly greater than σ_2/σ_1 (paired t-test, $P < 0.05$), further confirming that these aggregates do not obey Hooke's law and in fact behave as liquids. In contrast RPSMCs obeyed Hooke's law. As is evident in Table 1, the ratio of σ_2/σ_1 is significantly greater than 1 and was not statistically different than that of F_2/F_1. To further demonstrate liquid-like behavior, we explored the relationship between surface tension (σ) and aggregate volume. As can be seen in Fig. 8, volume is independent of sigma for RPF cells (red regression line, $r^2 = 0.002$), whereas there appears to be some dependence of sigma on volume for RPSMCs (blue regression line, $r^2 = 0.146$). These data further confirm that RPF aggregates behave in a liquid-like manner, whereas those of RPSMCs appear to behave more as elastic solids. Only those mesurements obtained from aggregates behaving as liquids would be used to calculate surface tension.

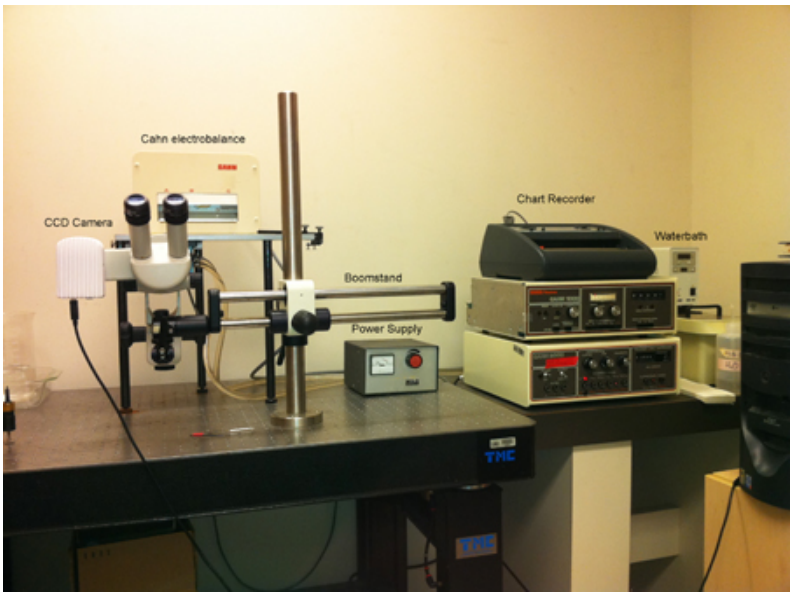

Figure 1. Overview of the tissue surface tensiometer.

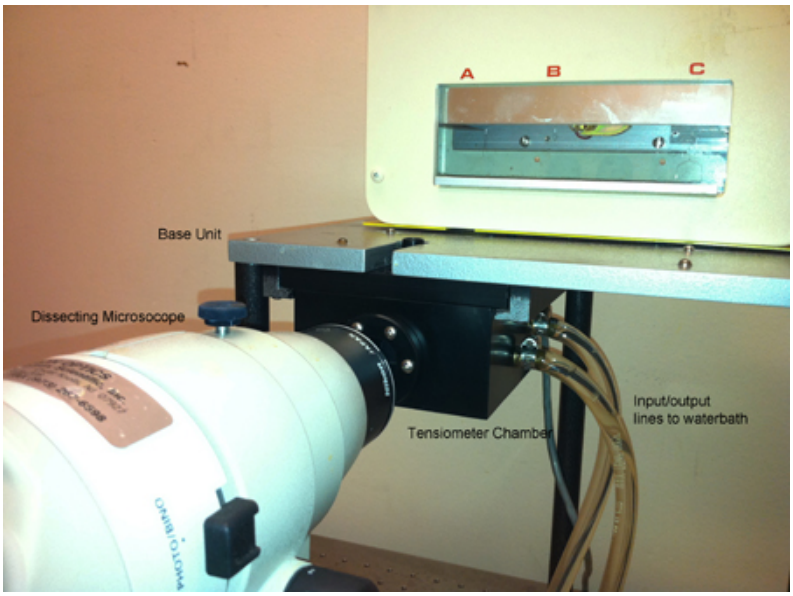

Figure 2. A more detailed view of the tensiometer chamber (right panel).

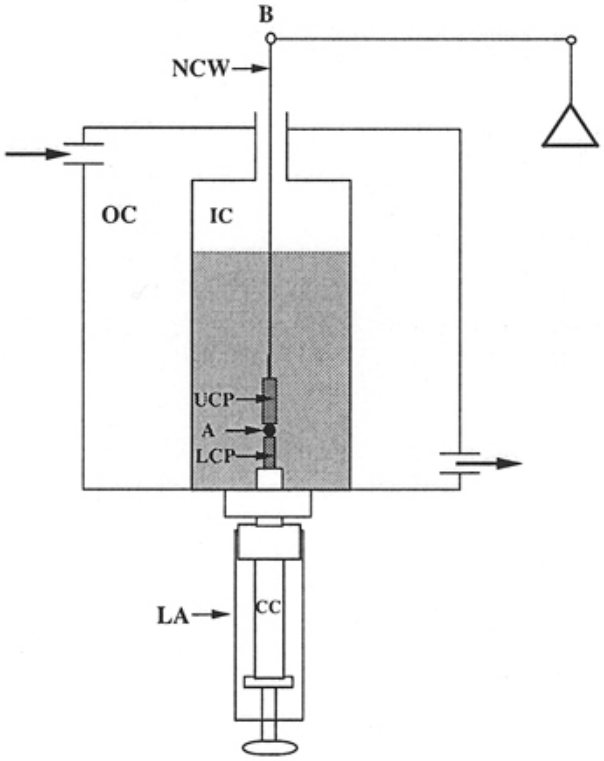

Figure 3. Schematic view of the tensiometer chamber.

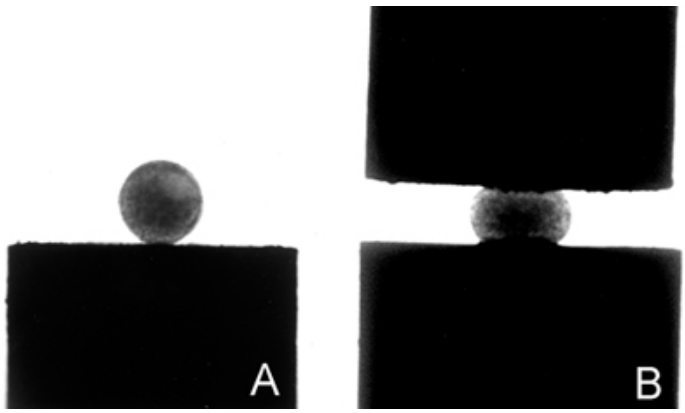

Figure 4. Images of uncompressed (A) and compressed (B) aggregates.

$$\sigma = \frac{F}{\pi R_3^2}\left(\frac{1}{R_1}+\frac{1}{R_2}\right)^{-1}$$

Figure 5. The Laplace Equation.

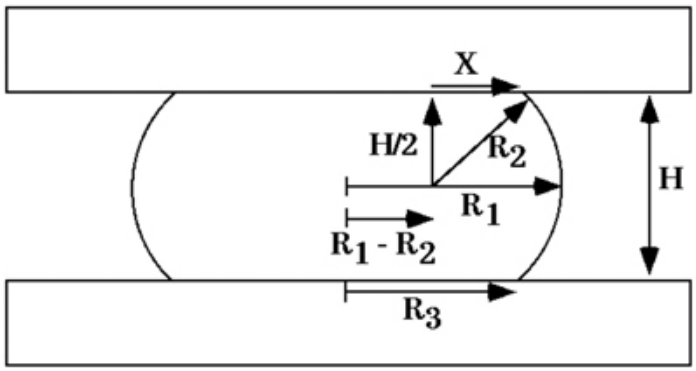

Figure 6. Diagram of a liquid droplet compressed between two parallel plates to which it adheres poorly, at shape equilibrium. R_1 and R_2 are the two primary radii of curvature, at the droplet's equator and in a plane through its axis of symmetry, respectively. R_3 is the radius of the droplet's circular area of contact with either compression plate. H is the distance between upper and lower compression plates. X is one side of a right-angled triangle with hypotenuse R_2 extending to a point of contact between the droplet's surface and either compression plate.

	σ_1(dynes/cm ± SEM)	σ_2(dynes/cm ± SEM)	Pσ_1 vs σ_2	$\sigma_{1,2}$(dynes/cm ± SEM)	σ_2/σ_1	F_2/F_1	Pσ_2/σ_1 and F_2F_1
RPF	22.6 ± 1.7	22.9 ± 1.4	> 0.05*	22.8 ± 1.1	1.04 ± 0.04	1.47 ± 0.06	< 0.05
RPSMC	15.0 ± 2.8	23.0 ± 3.2	0.039	NA	1.9 ± 0.3	1.6 ± 0.1	0.16*

Figure 7. TST measurements and confirmation of aggregate liquidity for aggregates of rat prostate fibroblasts and smooth muscle cells.

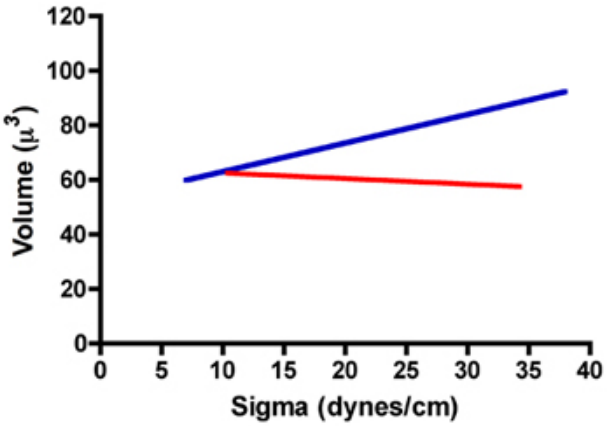

Figure 8. Relationship between sigma and volume for aggregates of RPF (red line) and RPSMCs (blue line).

Discussion

Measuring aggregate cohesion by TST is relatively straightforward. There are, however, key steps that must be mastered in order to generate useable TST data; 1) aggregates must be "healthy". This can be controlled by ensuring that aggregate formation begins with cells that are at optimal confluence prior to detachment. Aggregate size and time in culture must also be controlled to minimize the development of a necrotic core within the aggregate; 2) Another parameter that can influence TST measurements is the degree of adhesion of the aggregate to the upper or lower compression plates. Accordingly, the optimal concentration of poly-HEMA used to coat the plates must be empirically determined for each type of aggregate; 3) While it is preferable that pre-compression aggregates should be as spherical as possible, it is not strictly necessary. Some aggregates, particularly ones that are held together weakly, tend not to form perfect spheres. The explanation for this is that in order to completely round-up cells must expend energy by moving and re-arranging. If the amount of energy required to round-up into a sphere exceeds the energy minimization of becoming spherical, the aggregates will tend to stall at some sub-spherical shape. In our experience, such aggregates upon becoming compressed, resist the compressive force to an extent that the sides of the aggregate form semi-circles, exactly as they would do if starting from a perfect sphere; 4) It is also important that the compression plates are parallel to one-another. This is best accomplished by ensuring that the nickel-chromium wire is straight and that the instrument is level and plumb. If these measures are adhered to, tissue surface tensiometry is relatively simple and can generate very useful information on mechanical properties of tissues and of their underlying molecular determinants.

Other methods for measuring aggregate cohesion exist, some that eliminate the need for specialized equipment such as the Cahn electrobalance. One such method aspirates a spheroid into a pipette of much smaller diameter than that of the spheroid, with a constant suction pressure. The viscoelastic properties of the tissue are deduced from the variation of the strain by measuring the change in length of the cellular material as it flows inside the pipette[18]. While useful, this method may have limitations as to the range of surface tensions in which it can be applied. Very weak aggregates would likely be destroyed as they are aspirated into the pipette, whereas aggregates that are held together very strongly may not be aspirated at all. Parallel plate compression has measured surface tensions as low as 0.33 ± 0.02 dynes/cm for zebrafish germ layer ectoderm treated with E-cadherin morpholino[3] to as high as 20.1 ± 0.5 dynes/cm for aggregates of embryonic chick limb bud mesoderm[2], demonstrating its general utility over a broad cohesion range for several embryonic systems.

Disclosures

No conflicts of interest declared.

References

1. Foty, R. A., Forgacs, G., Pfleger, C. M. & Steinberg, M. S. Liquid properties of embryonic tissues: Measurement of interfacial tensions. *Phys Rev Lett* **72**, 2298-2301 (1994).
2. Foty, R. A., Pfleger, C. M., Forgacs, G. & Steinberg, M. S. Surface tensions of embryonic tissues predict their mutual envelopment behavior. *Development* **122**, 1611-1620 (1996).
3. Schotz, E.-M. *et al*. Quantitative differences in tissue surface tension influence zebrafish germ layer positioning. *HFSP Journal* **2**, 42-56. (2008).
4. Jia, D., Dajusta, D. & Foty, R. A. Tissue surface tensions guide *in vitro* self-assembly of rodent pancreatic islet cells. *Dev Dyn* **236**, 2039-2049 (2007).
5. Schwarz, M. A., Zheng, H., Legan, S. & Foty, R. A. Lung Self-Assembly is Modulated by Tissue Surface Tensions. *Am J Respir Cell Mol Biol*, doi:2009-0309OC [pii] 10.1165/rcmb.2009-0309OC (2010).
6. Ryan, P. L., Foty, R. A., Kohn, J. & Steinberg, M. S. Tissue spreading on implantable substrates is a competitive outcome of cell-cell vs. cell-substratum adhesivity. *Proc Natl Acad Sci U S A* **98**, 4323-4327. (2001).
7. Foty, R. A. & Steinberg, M. S. The differential adhesion hypothesis: a direct evaluation. *Dev Biol* **278**, 255-263 (2005).
8. Robinson, E. E., Foty, R. A. & Corbett, S. A. Fibronectin matrix assembly regulates alpha5beta1-mediated cell cohesion. *Mol Biol Cell* **15**, 973-981, doi:10.1091/mbc.E03-07-0528 E03-07-0528 [pii] (2004).

9. Robinson, E. E., Zazzali, K. M., Corbett, S. A. & Foty, R. A. alpha5beta1 integrin mediates strong tissue cohesion. *J Cell Sci* **116**, 377-386. (2003).
10. Winters, B. S., Raj, B. K., Robinson, E. E., Foty, R. A. & Corbett, S. A. Three-dimensional culture regulates Raf-1 expression to modulate fibronectin matrix assembly. *Mol Biol Cell* **17**, 3386-3396, doi:E05-09-0849 [pii] 10.1091/mbc.E05-09-0849 (2006).
11. Caicedo-Carvajal, C. E., Shinbrot, T. & Foty, R. A. Alpha5beta1 integrin-fibronectin interactions specify liquid to solid phase transition of 3D cellular aggregates. *PLoS One* **5**, e11830, doi:10.1371/journal.pone.0011830 (2010).
12. Foty, R. A. & Steinberg, M. S. Measurement of tumor cell cohesion and suppression of invasion by E- or P-cadherin. *Cancer Res* **57**, 5033-5036. (1997).
13. Foty, R. A., Corbett, S. A., Schwarzbauer, J. E. & Steinberg, M. S. Dexamethasone up-regulates cadherin expression and cohesion of HT-1080 human fibrosarcoma cells. *Cancer Res* **58**, 3586-3589. (1998).
14. Winters, B. S., Shepard, S. R. & Foty, R. A. Biophysical measurement of brain tumor cohesion. *Int J Cancer* **114**, 371-379, doi:10.1002/ijc.20722 (2005).
15. Foty, R. A., Cummings, K. B. & Ward, S. Tissue surface tensiometry: a novel technique for predicting invasive potential of prostate tumors based on tumor cell aggregate cohesivity *in vitro*. *Surgical Forum L*, 707-708 (1999).
16. Folkman, J. & Moscona, A. Role of cell shape in growth control. *Nature* **273**, 345-349 (1978).
17. Foty, R. A., Forgacs, G., Pfleger, C. M. & Steinberg, M. S. Liquid properties of embryonic tissues: Measurement of interfacial tensions. *Physical Review Letters* **72**, 2298-2301. (1994).
18. Guevorkian, K., Colbert, M. J., Durth, M., Dufour, S. & Brochard-Wyart, F. Aspiration of biological viscoelastic drops. *Phys Rev Lett* **104**, 218101 (2010).

